

EgoSonics: Generating Synchronized Audio for Silent Egocentric Videos

Aashish Rai

Srinath Sridhar

Brown University

<https://ivl.cs.brown.edu/research/egosonics>

Abstract

We introduce EgoSonics, a method to generate semantically meaningful and synchronized audio tracks conditioned on silent egocentric videos. Generating audio for silent egocentric videos could open new applications in virtual reality, assistive technologies, or for augmenting existing datasets. Existing work has been limited to domains like speech, music, or impact sounds and cannot capture the broad range of audio frequencies found in egocentric videos. EgoSonics addresses these limitations by building on the strengths of latent diffusion models for conditioned audio synthesis. We first encode and process paired audio–video data to make them suitable for generation. The encoded data is then used to train a model that can generate an audio track that captures the semantics of the input video. Our proposed SyncroNet builds on top of ControlNet to provide control signals that enables generation of temporally-synchronized audio. Extensive evaluations show that our model outperforms existing work in audio quality, and in our proposed synchronization evaluation method. Furthermore, we demonstrate downstream applications of our model in improving video summarization.

1. Introduction

As humans, we have the ability to watch a silent video and imagine the sounds that could be accompanying it. We use visual cues, such as the swaying of branches or the flowing of water, to conjure up the sounds of a tree or river. Machines with such capabilities could have potentially transformational applications in the movie industry, virtual reality, gaming, and in assisting people with disabilities. Although we now have models that can generate photorealistic videos from text [10, 18, 29, 42], these models cannot yet synthesize corresponding synchronized audio.

Recently, we have seen a surge in multimodal models [6, 14, 19, 25, 26, 30] that can learn mappings between domains such as text-to-images, image-to-text, text-to-video, and text-to-audio [50, 54]. Multimodal models that operate with audio have thus far been primarily limited to image-to-audio (I2A) [23, 41] or audio-to-image (A2I) [47] synthesis. There

are relatively fewer works that explore the video-to-audio (V2A) or audio-to-video (A2V) problems due to the complex temporal and spatial understanding required. Thus, these works have been limited to domains like speech [4, 7, 21], music [45], or impact sounds [46]. Furthermore, existing models have short video contexts (1–4 frames [11, 22, 30, 41]), cannot produce audio that is synchronized with the input video, and are limited to audio frequencies of less than 8 KHz [22, 30, 41].

In this paper, we address the problem of **generating synchronized audio tracks** for silent everyday videos. Specifically, we focus on *egocentric* videos – videos that are captured using head- or body-worn cameras providing a first-person viewpoint. Our focus on egocentric videos is driven by potential applications arising from the gaining popularity of wearable and assistive technologies [5, 28, 31, 32]. For instance, wearable virtual reality devices can generate immersive 3D visual environments, but audio and sounds are harder to synthesize [5, 8]. Existing egocentric datasets [9, 17] often lack audio due to privacy concerns, technical constraints, or other design factors. Even if video generative models [10, 18, 29] can synthesize very realistic egocentric videos, they cannot yet generate the corresponding synchronized sounds, thus limiting their applications.

We present **EgoSonics**, a method that can generate synchronized audio tracks conditioned on silent egocentric videos. We build upon the state-of-the-art generation capabilities of Latent Diffusion Models [20, 38, 44] to generate realistic audio tracks that are not only semantically meaningful to the visual content of videos but also synchronized to events in them (see Figure 1). We cast audio generation as an image generation problem by operating on the Short-Time Fourier Transform “image” [33] of raw audio signals that are time-aligned with the input video. We introduce the **SyncroNet** module which builds upon ControlNet [53] to consume videos in the form of temporally-stacked images. The use of temporally-aligned and encoded audio-video pairs enables SyncroNet to learn correspondences through self- and cross-attention. We then use Stable Diffusion model [38] to generate audio spectrograms conditioned on the control signals from *SyncroNet* and the video embedding.

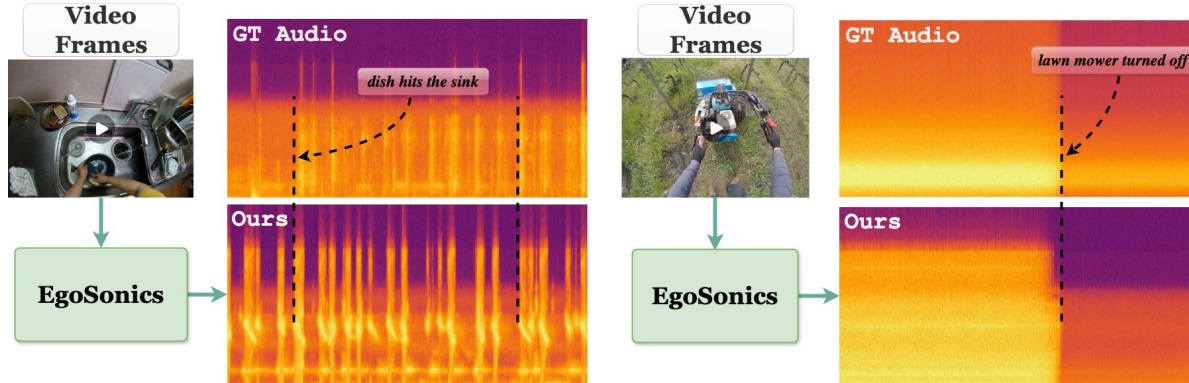


Figure 1. We present **EgoSonics**, a method to synthesize audio tracks conditioned on silent in-the-wild egocentric videos. Our method operate on videos at 30 fps, and can synthesize audio that is semantically meaningful and synchronized with events in the video (“dish hits the sink” or “lawn mower turned off”). We also propose a new method to evaluate audio-video synchronization quality.

Different from previous works, EgoSonics operates on videos captured at 30 frames per second (fps) to accurately synchronize the synthesized audio, allowing us to effectively capture auditory events in the video. Unlike previous work that are often limited to audio frequencies of less than 8 KHz, we operate on a broader set of frequencies (upto 20 KHz) – an important factor to consider when dealing with egocentric day-to-day activities that contain useful frequencies of up to 16 KHz. To improve quality even further, we use a learned audio upsampler that super-resolves the generated audio. Our method achieves state-of-the-art results in generating high quality, semantically meaningful, and synchronized audio on the Ego4D dataset [17].

Measuring synchronization between the synthesized audio and the input video is a challenging problem with no standardized metric in the community. Therefore, we provide a new way to accurately measure audio-visual (AV) synchronization by extracting AV features through a Vision Transformer (ViT) and training an MLP to learn the alignment between these features in a contrastive manner. We outperform existing methods including Im2Wav [41], Diff-Foley [30], and Make-an-audio [22] in audio quality and synchronization. In addition, we also show EgoSonics can improve video summarization results on egocentric data. To sum up our main contributions:

- We propose **EgoSonics**, a method to generate semantically meaningful and synchronized audio for everyday silent egocentric videos.
- We propose the **SyncroNet** module that can extract the temporal information from a video at 30 fps and produce control signals to enable conditional audio generation with better synchronization.
- To overcome the limitations of existing audio-video synchronization metrics, we propose a new method to evaluate synchronization accuracy.

We highly encourage readers to see the accompanying videos to fully appreciate our results.

2. Related Works

Generative Models and Multimodal Learning. Diffusion Models [20, 38, 44] have demonstrated remarkable efficacy in a multitude of generative tasks, spanning image generation, audio synthesis, and video creation. Among these, latent diffusion models like Stable Diffusion (SD) [38] stand out for their ability to perform both forward and reverse processes within the latent space of data, leading to efficient computation and expedited inference. Notably, SD is engineered to execute inference even on standard personal laptop GPU, making it a practical choice for a wide array of users. Alongside diffusion models, other generative architectures such as Variational Autoencoders (VAEs) [3, 48], Generative Adversarial Networks (GANs), and Autoregressive models have also made significant strides in various creative domains, each with their own strengths and uses.

With the recent developments in the generative models, we have seen a significant rise in multimodal learning. Text guided synthesis has seen a rapid development in the last few years. The state-of-the-art DALL-E [2, 37] can generate realistic images given natural language text queries by encoding images into latent tokens. Other recent text-to-image (T2I) models include [15, 27, 51, 52]. The progress has also been made in text-to-video, where papers like Make-a-Video [42] uses text-to-image to sample an image and then uses the temporal understanding of real-world videos to translate the sampled image into a video. Very recently, we have also seen realistic text-to-video synthesis from SORA, VEO [10, 29]. Text-to-audio has also seen some progress in the past few years. However, due to the lack of large amount of text-to-audio datasets, we don’t see as much progress as in T2I. Works like [24, 40, 49], use datasets like AudioSet [16] for training and are able to generate music from text.

Audio-Visual Learning. The exploration of audio-visual cross-modal generation encompasses two primary directions: vision-to-sound and sound-to-vision generation. Vision-to-sound tasks have been studied in contexts such as instrument/music and speech generation [6, 19, 45]. Recent efforts by Luo et al. [30], Iashin et al. [23], and Huang et al. [22] aimed to broaden the scope by conditioning sound generation on videos from diverse categories. Majumder et al. [31] tries to learn AV correspondance for active speaker detection and spatial audio denoising. However, our approach surpasses previous limitations, enabling the generation of plausible and synchronized audios from a wide range of everyday activities, including but not limited to *cooking, laundry, carpentry, running, placing items*, etc. Unlike earlier methods, our model produces high-quality audio closely related to the input audio. Existing V2A methods struggle with synchronization as they lack audio-related information in pretrained visual features, limiting the capture of intricate audio-visual correlations.

Im2Wav [41] generates an audio given an image. It uses a two-transfer model and uses CLIP [36] image embeddings are the conditional signal to guide the low-level and up-level transformers. Make-An-Audio [22] is a text-to-audio generation model that leverages a prompt-enhanced diffusion model. It uses a pair of audio encoder-decoder network to convert the audio spectrogram into the rich feature space where the diffusion process is applied. Cross-attention is applied with the text embeddings coming from a text encoder. It can generate I2A as they leveraged the fact that CLIP image and text embeddings share the same latent space. For V2A, the model samples 4 frames from the video, uses a pooling layer to get an average embedding and then use it to condition the audio generation.

Both the Im2Wav [41] and Make-an-audio [22] lacks synchronization in generated audio, as neither single image nor four frames are enough to get semantic and contextual information from the activity being performed in the video and generate the synchronized audio. These methods may work for videos with less difference between different frames, eg., *video of an ocean, a car on the road, musical instruments*, etc. But they are not suitable for activity videos where even two consecutive frames might differ and contain rich semantic changes. For video condition sampling, Im2Wav takes the mean of all the video frame embeddings, and uses it to guide the audio generation. However, this loses the temporal understanding of the video and can only give global guidance for audio generation.

The closest paper to ours is Diff-Foley [30], which tries to synthesize synchronized audio given a muted video using the a contrastive audio-visual pretraining (CAVP) framework. CAVP tries to align the audio and video features using contrastive learning by bringing similar samples closer and vice-versa. The CAVP-aligned video features are later used

to train a latent diffusion model to generate audio. However, the quality of audio generated by the framework is sub-optimal - a result of using lower audio sampling rate and smaller mel basis to fit more data into a smaller spectrogram. Also, in-the-wild testing of the framework on day-to-day activities generate out-of-context and non-synchronized audios. It only uses four frames per second in a video, thereby limiting the amount of information that can be captured from a video.

3. Method

Given an audio-video pair (A, V) , we want to learn a conditional generative model to synthesize audio waveforms $A \in \mathbb{R}^{T' \cdot f_{sa}}$, conditioned on a video $V \in \mathbb{R}^{T' \cdot f_{sv} \times W \times H \times 3}$, where, T' is the duration of clip in seconds, f_{sa} is the audio sampling rate (generally 16 KHz–48 KHz), f_{sv} is the frame rate of video (generally 30, 45, 60, 90 fps), $W \times H \times 3$ is the shape of RGB video frame. Learning a conditional model to generate a high-dimensional audio waveform of size $T \times f_{sa}$ is non-trivial and cumbersome [24, 30, 41], so we first encode the audio (E_A) and video (E_V) for efficient learning.

Our goal then is to train a conditional generative model that can generate audio encodings E_A given the video embedding E_V with per-frame synchronization - $\mathcal{P}(E_A|E_V)$. Figure 2 shows our approach that consists of a two-step process, where the first stage generates control signals to guide the conditional generative model $\mathcal{P}(E_A|E_V, C)$, where $C := \{c^{(n)}\}_{n=1}^N$ are the control signals. The control signals provide pixel-level local guidance to a diffusion-based generative model. We describe each component of our architecture below.

3.1. Audio/Video Preprocessing

Audio Encoding and Pruning. To compactly encode audio, we use the widely-adopted using Short-Time Fourier Transform (STFT) [33] representation. A spectrogram, $E_A \in \mathbb{R}^{T \times D}$ is an “image” of the audio frequencies over time, obtained through the Fourier transform of the audio signal. The X-axis of audio spectrograms generally represents time, while the Y-axis represents frequencies at each time step. Since we cast audio as spectrogram images, we can use the image generation capabilities of diffusion models to generate audio.

Large datasets like Ego4D [17] may contain videos where audio is from background activities (e.g., traffic) rather than foreground visual cues. To avoid overfitting to such uninformative audio signals, we only select useful and relevant clips by picking non-overlapping video clips based on a threshold Root Mean Square (RMS) value of the audio waveform. The audio waveforms $A \in \mathbb{R}^{T' \cdot f_{sa}}$ are converted to spectrograms $E_A \in \mathbb{R}^{T \times D}$. More details about audio preprocessing and selection are given in the supplementary.

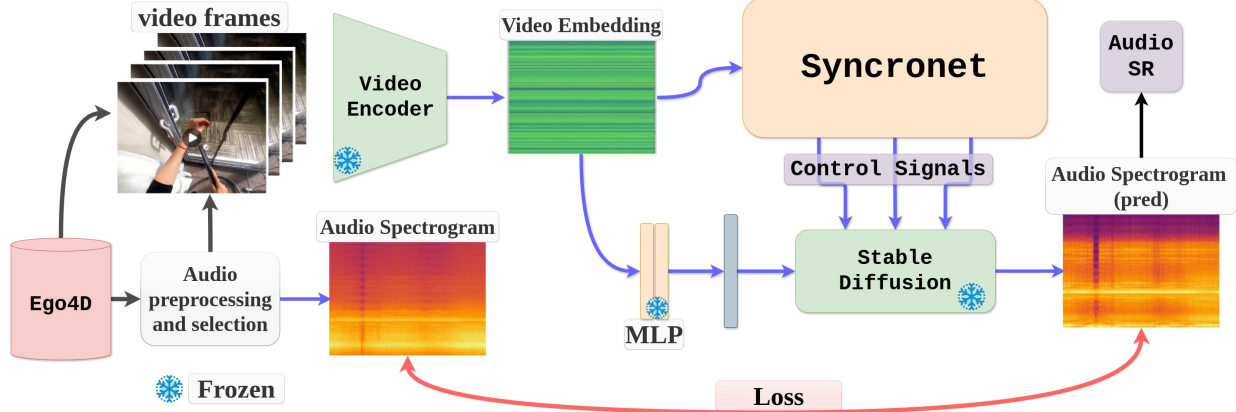


Figure 2. The overall architecture of our proposed method - EgoSonics. The input video frames are encoded through a video encoder to get video embedding E_V . This video embedding goes to the *SyncroNet* 3.3 which generates several control signals to control the generation of audio spectrograms by providing pixel-level temporal control to a pre-trained Stable Diffusion (SD) 3.2. An MLP translates the video embedding into text embedding c_t for SD. The loss between the ground truth audio spectrogram E_A and predicted E'_A is used to train the *SyncroNet*. Finally, as a post processing step, generated audio is upsampled using Audio SR module.

Video Encoder. To encode videos, we repurpose the CLIP [36] image encoder which is trained on a large dataset of images and corresponding text descriptions. CLIP allowed us to generate a rich video embedding capable of capturing subtle changes in different frames of the video.

Given a video $V \in \mathbb{R}^{t \cdot f_{sv} \times W \times H \times 3}$ of duration t seconds, recorded at f_{sv} frames per second (fps), our goal is to generate a video embedding $E_V \in \mathbb{R}^{T \times h}$, where $T = t \times f_{sv}$ and h is the size of feature vector for each frame f_i in the video. We use CLIP to capture semantically rich and meaningful information from each frame of the video. The image encoder converts each frame of the video into a feature vector $E_V^i = \mathcal{F}_V(f_i)$. We stack all such feature vectors for all the frames in the video to get the final feature representation of the video $E_V = \{E_V^i\}_{i=1}^{N=t \cdot f_{sv}}$. This feature representation of the video can be interpreted as an image of size $T \times h$ as shown in Figure 2.

Images sharing the same embedding space as text is crucial for our model design as explained in the further sections. $E_V = \{E_V^i\}_{i=1}^{N=t \cdot f_{sv}} = \{\mathcal{F}_V(f_i)\}_{i=1}^N = \{\mathcal{F}_{V-CLIP}(f_i)\}_{i=1}^N$.

We set the audio sampling rate and video frame rate such that they have the same T .

3.2. Diffusion Model for Audio Synthesis

Since we represent audio as spectrograms, we can build on the strengths of Latent Diffusion Models [38] for high-quality audio synthesis. LDMs (e.g., Stable Diffusion) use pretrained Variational Autoencoder [13] to convert the original image $x \in \mathbb{R}^{H \times W \times 3}$ into a compact latent representation $z \in \mathbb{R}^{h \times w \times c}$, where the forward and reverse diffusion processes are applied [38]. The decoder then converts the compact latent representation back to pixels.

Stable Diffusion (SD) can use text prompt conditioning to guide the image generation. The text prompts are given to a pretrained CLIP text encoder to generate a text embedding $c_t \in \mathbb{R}^{77 \times 768}$, which is also given to the UNet encoder of SD. Thus, the overall objective function for SD becomes:

$$\mathcal{L}_{LDM} := \mathbb{E}_{\epsilon(x), \epsilon \sim \mathcal{N}(0,1), t, c_t} [\|\epsilon - \epsilon_\theta(z_t, t, c_t)\|_2^2] \quad (1)$$

where, $\epsilon_\theta(\cdot, t)$ is a time-conditional U-Net [39] model, $\mathcal{N}(0, 1)$ is the Normal distribution, z_t is the latent code, and c_t is the text embedding.

In our model, we replace the text prompt from the SD with the video embedding E_V . The mean of all the image embeddings $\frac{1}{N} \sum_{i=1}^N E_V^i$ is passed through a small MLP to map it to the corresponding c_t providing some contextual information to the UNet encoder blocks of the SD. As our video embeddings E_V are also generated using CLIP, it makes it easier to reuse existing SD models that already operate with CLIP embeddings. More details about the MLP are given in the supplementary.

To generate synchronized audio from video, we use an additional conditioning C coming from our *SyncroNet* model. This additional conditioning provides the pixel-level control (i.e., **local guidance**) and acts as a local conditioning mechanism between E_V and the SD's feature space. Thus, the final SD model is conditioned on mean E_V providing some global context to the UNet encoder, and C for adding local pixel-level control to the UNet based decoder for controlled audio synthesis (see Figure 2(left)). Thus, the final overall objective function for the training becomes:

$$\mathcal{L}_{LDM} := \mathbb{E}_{\epsilon(x), \epsilon \sim \mathcal{N}(0,1), t, E_V, C} [\|\epsilon - \epsilon_\theta(z_t, t, E_V, C)\|_2^2]. \quad (2)$$

Next section describes how we use E_V for additional conditioning C using the *SyncroNet* model.

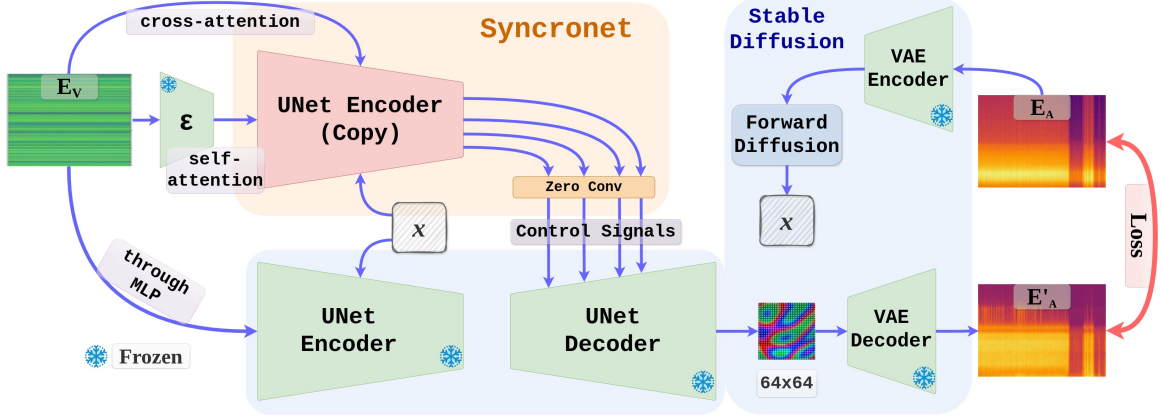


Figure 3. Figure describes the training of SyncroNet model. A trainable copy of Stable Diffusion’s UNet encoder generates control signals through zero convolution layers, providing pixel-level control to the pretrained UNet Decoder model. The UNet decoder generates a 64×64 encoded feature map, which goes through VAE decoder to generate the predicted audio spectrogram E'_A .

3.3. Time-Aware Audio Control using SyncroNet

We propose an strategy to learn the correspondences between the input video embeddings and the audio frequencies for every time step t using **SyncroNet**. SyncroNet builds upon ControlNet [53], a modal to enhance large pretrained text-to-image diffusion models with spatially localized, task specific image conditions for pixel-level control. Originally, ControlNet was designed for a variety of spatial conditions like Canny edges, Hough lines, user scribbles, human key points, segmentation maps, shape normals, depths, and cartoon line drawings. ControlNet works by processing these spatial conditioning and injecting additional control signals to the pretrained diffusion models.

SyncroNet enhances the original ControlNet architecture to replace the text embedding c_t with the video embedding E_V , and uses self-attention and cross-attention mechanism to inject time-aware control signals to the Stable Diffusion’s UNet Decoder (see Figure 3). As a first step, we make a trainable copy of the entire UNet based encoder of SD along with the middle block and initialized them with the pretrained weights of SD 2.1. The goal here is to use this trainable encoder to generate control signals that can be plugged into the pretrained SD’s UNet decoder blocks providing pixel-level control to output (see Fig. 3). The trainable copy is connected to the frozen SD through zero convolution layers to avoid any influence of noisy control signals during the start of the training.

As shown in Fig. 4, first, we transfer the input video embedding E_V to a more rich 64×64 feature space through a pretrained encoder $\epsilon(\cdot)$, where it’s added to the input noisy data sample x . $h = x + \epsilon(E_V)$. The added sum is further enriched by passing them through a self-attention block.

$$Self - Attn(Q_h, K_h, V_h) = Softmax\left(\frac{Q_h K_h^T}{\sqrt{d_K}}\right)V_h \quad (3)$$

$$h = h + Self - Attn(Q_h, K_h, V_h)$$

where, Q_h, K_h, V_h represents the Query, Key, and Value matrices derived from h .

This would help incorporate contextual information from spatially varying signals in the same feature space, allowing the model to generate quite relevant audio.

However, this alone is not sufficient to capture the fast temporal changes in the video. Thus, alongside self-attention with the encoded video embedding $\epsilon(E_V)$, we also apply the cross-attention with the original video embedding E_V to guide the audio spectrogram generation directly with the changes in time domain. This will help the model effectively learn the synchronization between the time domain and the rich feature space of Stable Diffusion. Also enabling the model avoid any inherited time-agnostic properties in the encoder

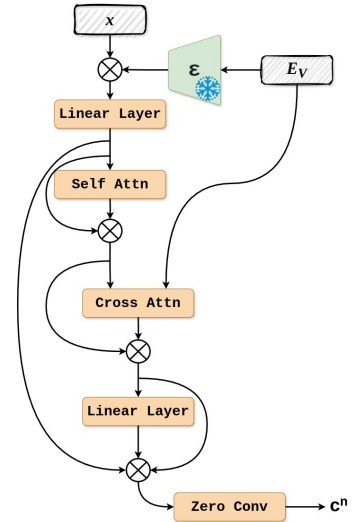


Figure 4. Self-attention is applied to the sum of encoded video embedding and the noisy input sample. Then the cross-attention is applied between E_V and the previous intermediate signal. Post which, they are passed through a linear layer followed by a zero convolution layer to get control signal c^n .

model of SD, which has never seen time aware data.

$$Cross - Attn(Q_h, K_V, V_V) = Softmax\left(\frac{Q_h K_V^T}{\sqrt{d_K}}\right)V_V \quad (4)$$

$$h = h + Cross - Attn(Q_h, K_V, V_V)$$

where, Q_h, K_V, V_V represents the Query, Key, and Value matrices derived from h and E_V , respectively. After passing through a *linear layer*, a *zero convolution* layer is applied to get the control signal c^n . This attention mechanism (Fig. 4) is applied to all the Spatial Transformers in the Stable Diffusion’s UNet encoder and middle blocks (7 in total). More details are given in the supplementary.

Similar to the original ControlNet model, the SyncroNet model \mathcal{S} generates 13 control signals using x and E_V . $C := \{c^n\}_{n=1}^{13} = \mathcal{S}(x, \epsilon(E_V), E_V)$. These control signals are added to the 12 skip-connections and 1 middle block of the Stable Diffusion’s UNet decoder block providing local pixel-level guidance.

3.4. Training and Inference

Before training SyncroNet, we train the video-to-text embedding MLP, and initialized SD 2.1, SyncroNet encoder $\epsilon(\cdot)$, and CLIP image encoder with their original pre-trained weights. All these module are kept frozen during the *SyncroNet* training.

For training SyncroNet first, the video frames are encoded using the video encoder. The video embedding is then given to the *SyncroNet* which generates control signals to guide the SD’s UNet decoder. The UNet decoder generates a 64×64 feature representation, which then goes to the VAE decoder to generate the audio spectrogram. The loss is applied between the generated audio spectrogram E'_A and the ground truth spectrogram E_A as shown in fig. 3. The SyncroNet training is carried out as per the objective mentioned in Eq. 5. Training of *SyncroNet* has been done using the same loss functions as ControlNet [53]. We use DDIM [20] for faster and consistent sampling. Upto 1000 time steps were used in the forward diffusion process, and 20 during the denoising. Training was done using AdamW optimizer with a learning rate of $1e - 4$ for 50 epochs.

During **inference**, the given video sampled at 30 fps is given to the CLIP video encoder to obtain an image-like video embedding. SyncroNet generates the control signals using this video embedding, which is then given to a DDIM sampler [20] which predicts the conditioned encoded feature map for audio spectrogram. This feature map is decoded using Stable Diffusion’s pretrained decoder to obtain the audio spectrogram synchronized with the input video. The pretrained audio super-resolution (ASR) model is used to enhance the generated audio quality and recover the losses occurred due to rescaling. More details on ASR are given in

the supplementary. We scale and invert this enhanced audio spectrogram using Griffin-Lim [33] algorithm to obtain the audio waveform of 10 seconds.

Video-Audio Alignment Score (VAAS) Inspired by [30], we propose a Video-Audio Alignment Score (VAAS) to compare the audio-visual alignment. As there is no standard benchmark to measure the alignment accuracy, we trained a classifier that uses ViT to extract the audio and video features and calculates the alignment between them. The classifier training dataset consists of three AV pairs - 50%, 25%, and 25%, respectively for pairs from the same video, pairs from different videos, and the pairs of the same video but temporally shifted by a random amount. Only the first 50% AV pair are considered as *True* during the training and the remaining 50% are considered *False*. The ViTs for extracting AV features share the same weights.

4. Experiments

The goal of our experiments is to compare the audio and synchronization quality of generated audio, justify and ablate key design decisions, and demonstrate the application of our method in improving video summarization.

Dataset. We use one of the largest audio-visual egocentric datasets, Ego4D [17], which consists of roughly 3600 hours of egocentric videos capturing various daily activities. However, not all videos in this dataset contain audio, and even those with audio do not always contain useful learnable information (e.g., background noise). Therefore, we focus on videos with useful learnable visual audio cues, and pick 10-second chunks as described in Section 3.1. After this process, we obtain around 150K videos with the corresponding audio. We use STFT [34] to convert these 10 seconds long audio waveform into spectrograms. We sampled the audio at 22 KHz to get $E_A \in \mathbb{R}^{430 \times 1024}$.

Experimental Setup. We train our model for 50 epochs on 8 Nvidia 3090 GPUs. Video embeddings and audio spectrograms are extracted from the 10-second clips and resized to 512×512 to ensure synchronization between video and audio modalities. We used the pretrained weights of CLIP Image encoder and used it to obtain E_V . SyncroNet is initialized with the pretrained SD’s UNet encoder weights, and the zero convolutions are initialized with zero weights to prevent issues in the generated results during initial iterations. We also use the same Classifier-Free Guidance Resolution Weighting scheme as proposed in [53].

Metrics. For quantitative evaluation, we have used the two standard Frchet Distance (FID) and Inception Score (IS) as used in most previous works [22, 30, 41]. FID is used to measure the distribution-level similarity with the dataset, IS is effective in measuring the sample quality and diversity.

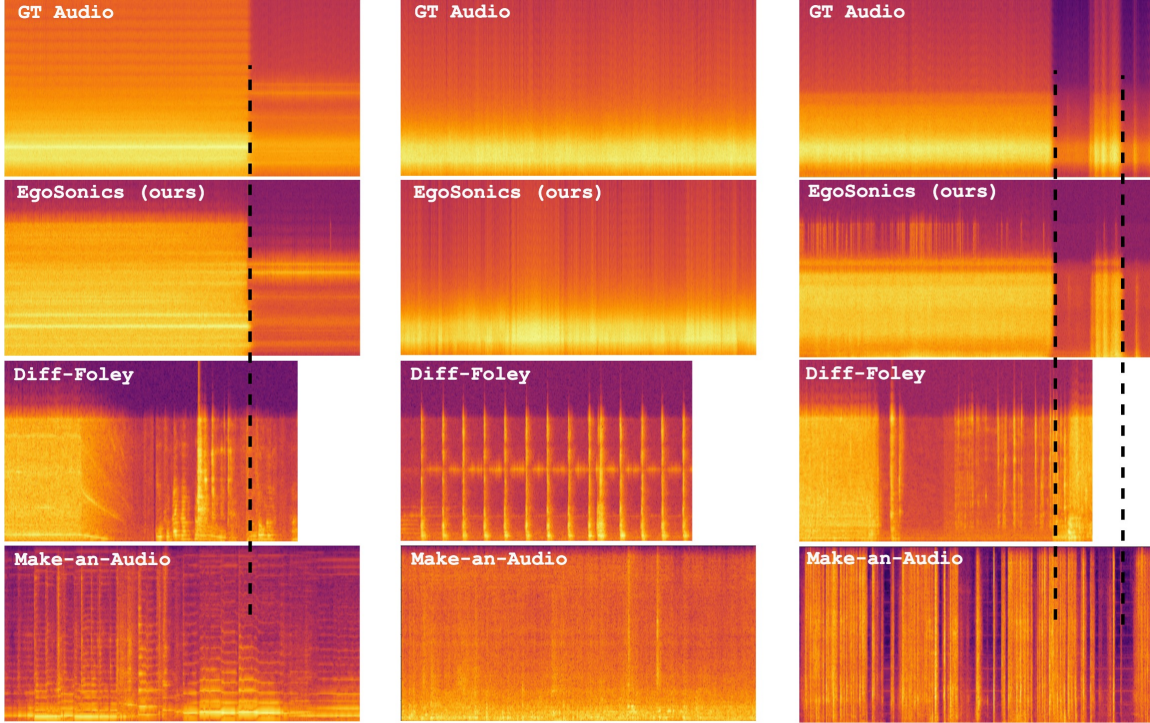


Figure 5. Figure compares how well each model can synchronize the generated audio with the GT audio. Our method can generate very synchronized audios with higher quality. On the other hand, Diff-Foley and Make-an-Audio fails to do so, and often fails to synthesize contextually correct audio. Diff-Foley can only synthesize 8 seconds long audio compared to 10 seconds for others.

Table 1. V2A generation results comparing various methods over 3 metrics (FID, IS, VAAS). We have also compared them against the audio sampling rate, maximum frequency support, spectrogram size used, the length of generated audio, and the number of video frames used for guidance. Our method, using 30 fps, sampled at highest frequency can generate the highest resolution spectrogram for a 10 seconds long audio. It also outperforms the existing V2A on FID, IS, and VAAS.

| Method | Audio SR | Max Freq. | Spec. Size | Audio Length | Video Frames | FID ↓ | IS ↑ | VAAS ↑ |
|------------------|----------|-----------|------------|--------------|--------------|--------------|--------------|--------------|
| Im2Wav | 16KHz | 8KHz | – | 5sec | 1 – 30fps | 91.73 | 19.15 | 59.24 |
| Make-an-Audio | 16KHz | 8KHz | 80 × 624 | 9 – 10sec | 1 – 4 | 83.72 | 22.14 | 64.57 |
| Diff-Foley | 16KHz | 8KHz | 256 × 128 | 8sec | 4fps | 76.92 | 37.92 | 78.19 |
| EgoSonics (ours) | 22KHz | 20KHz | 512 × 512 | 10sec | 30fps | 41.14 | 54.41 | 92.77 |

The proposed VAAS metrics is essential to measure how well the generated audio is synchronized with the video. Thus, it captures the alignment between the audio and video features.

4.1. Qualitative and Quantitative Comparisons

Qualitative results generated from our pipeline are shown in Figure 1 (please also see supplementary video). From the results, we see that our method not only generates good quality audio spectrograms corresponding to video activities but also achieves synchronization as depicted by the dotted lines where some distinct event in the video. Moreover, we observe that our method implicitly learns to suppress background noise and only generate sounds of interest, thus acting as an **Implicit Noise Removal** technique. This is the main reason why all the ground truth (GT) audios contain

a lot of soft frequency components, but audio generated from our method does not. More results are presented in the supplementary.

The quantitative results of our method are presented in Table 1. Our proposed method generating 10 seconds long audio with frequencies upto 20 KHz is able to generate better results than all the baselines in FID and IS measurement. Using 30 frames per second from the input video helped us in better alignment of the generated audio, thus, achieving a 14% increase in Video-Audio Alignment Score (VAAS).

4.2. Video Summarization

To demonstrate applications of our method beyond just audio generation, we show that it can be used to improve the quality of video summarization. Video summarization

Table 2. Comparing the effect of using audio generated from different methods on improving video summarization task. It is interesting to note that, even the un-synchronized audios generated from our model have sufficient contextual information to outperform the existing methods.

| Method | Cosine Similarity \uparrow |
|--------------------------|------------------------------|
| Without Audio | 0.67 |
| GT Audio | 0.81 |
| Im2Wav | 0.57 |
| Make-an-Audio | 0.68 |
| Diff-Foley | 0.71 |
| EgoSonics w/o Cross-Attn | 0.72 |
| EgoSonics (ours) | 0.76 |

[1] involves providing a short summary of a scene in a given video via understanding the video frames. We leverage the fact that audio provides additional cues about the scene [35, 43] through the easily identifiable sounds associated with each activity. Our aim is to incorporate the audio generated from our method alongside video encoding, and observe an improvement in the accuracy of video summarization. This will highlight the effectiveness of our method in generating relevant sounds capturing high-order details of the scene. More details about the video summarization architecture are presented in the supplementary. Table 2 compares the cosine similarity between the text embedding predicted from the video summarization model and the GT text embedding we generated using Ego4D narrations [17] for various methods. It can be seen that the audio generated by EgoSonics can significantly help in predicting the correct text embedding and outperforms existing V2A methods.

Table 3. Comparing the performance of our model against various changes, including removing the Synchronet model, removing cross-attention in Synchronet, and using video guidance at different fps.

| Method | FID | VAAS |
|--------------------------|--------------|--------------|
| EgoSonics w/o Synchronet | 150.28 | — |
| EgoSonics w/o Cross-Attn | 34.33 | 72.83 |
| EgoSonics @4 fps | 37.18 | 84.97 |
| EgoSonics @15 fps | 40.72 | 89.39 |
| EgoSonics @30 fps | 41.14 | 92.77 |

4.3. Ablation Study

w/o SyncroNet. Our method achieves better audio-visual synchronization since we use 30 frames per second to make SyncroNet learn the per-frame correspondences between audio and video. Here, we analyzed the effect of removing SyncroNet completely and solely using the mean video embedding to guide the Stable Diffusion. From the results, it can be seen that there is a significant drop in FID meaning

the pre-trained Stable Diffusion cannot synthesize the good quality audio spectrograms. Consequently, SD is not able to generate conditional audio and lacks synchronization.

w/o Cross-Attention in SyncroNet. Now, we also analyzed the effect of removing Cross-Attention with the video embedding E_V in SyncroNet and just using Self-Attention as given in Eqn. 3. From Table 3, it’s clear that our method is able to synthesize good quality audio spectrograms as the FID score is good. However, the poor alignment score indicates that the local pixel level alignment control to achieve synchronization is coming from the control signals through cross-attention with the video embedding E_V in the time domain.

Effect of Video Rate on Alignment. Unlike previous methods that use an average video embedding, or 1-4 fps for conditioning the audio, we used 30 fps to extract the temporal information from the video for guidance. In this section, we analyzed the impact of using 30 frames on AV synchronization. We compared the performance of SyncroNet at different fps including 4 fps used by the current SOTA Diff-Foley [30]. From Table 3, it can be seen that our method is not only able to generate good quality audio spectrograms, but also able to generate a VAAS score of 85. However, as we increase the fps to 15, the alignment score increases to 89, and then to 92.77 with 30 fps.

5. Conclusion

In this paper, we build a novel audio-visual framework called EgoSonics. Much like how humans effortlessly connect sound with visual stimuli, EgoSonics has the ability to predict synchronized audio for muted Egocentric videos. Leveraging a streamlined architecture that incorporates generation capabilities of Stable Diffusion, EgoSonics holds promise for various applications. The proposed Synchronet can generate control signals from input video frames to provide pixel-level control to Stable Diffusion. Furthermore, we showcased our method’s superior performance over existing methods and illustrate how this approach can enhance downstream applications like video summarization.

Limitations and Future Work. Although, EgoSonics can generate good quality audio for egocentric videos, there are a few limitations to our approach. One of the things we observed in some of our generated samples is the misalignment due to the lack of rich visual information, which might result from occlusions. We are also limited by the amount of data available for training. For example, since there are a very few samples of musical instruments in the Ego4D dataset, our model doesn’t perform very well on such videos. We believe that such challenges can be solved by training our model on a large amount of dataset comprising millions of audio-video pairs.

References

- [1] Evlampios Apostolidis, Eleni Adamantidou, Alexandros I Metsai, Vasileios Mezaris, and Ioannis Patras. Video summarization using deep neural networks: A survey. *Proceedings of the IEEE*, 109(11):1838–1863, 2021. 8
- [2] James Betker, Gabriel Goh, Li Jing, Tim Brooks, Jianfeng Wang, Linjie Li, Long Ouyang, Juntang Zhuang, Joyce Lee, Yufei Guo, et al. Improving image generation with better captions. *Computer Science*. <https://cdn.openai.com/papers/dall-e-3.pdf>, 2(3):8, 2023. 2
- [3] Taylan Cemgil, Sumedh Ghaisas, Krishnamurthy Dvijotham, Sven Gowal, and Pushmeet Kohli. The autoencoding variational autoencoder. *Advances in Neural Information Processing Systems*, 33:15077–15087, 2020. 2
- [4] Changan Chen, Alexander Richard, Roman Shapovalov, Vamsi Krishna Ithapu, Natalia Neverova, Kristen Grauman, and Andrea Vedaldi. Novel-view acoustic synthesis. In *Proceedings of the IEEE/CVF Conference on Computer Vision and Pattern Recognition*, pages 6409–6419, 2023. 1
- [5] Changan Chen, Kumar Ashutosh, Rohit Girdhar, David Harwath, and Kristen Grauman. Soundingactions: Learning how actions sound from narrated egocentric videos. *arXiv preprint arXiv:2404.05206*, 2024. 1
- [6] Lele Chen, Sudhanshu Srivastava, Zhiyao Duan, and Chenliang Xu. Deep cross-modal audio-visual generation. In *Proceedings of the on Thematic Workshops of ACM Multimedia 2017*, pages 349–357, 2017. 1, 3
- [7] Jeongsoo Choi, Joanna Hong, and Yong Man Ro. Diffv2s: Diffusion-based video-to-speech synthesis with vision-guided speaker embedding. In *Proceedings of the IEEE/CVF International Conference on Computer Vision*, pages 7812–7821, 2023. 1
- [8] Gustavo Corrêa De Almeida, Vinicius Costa de Souza, Luiz Gonzaga Da Silveira Júnior, and Maurício Roberto Veronez. Spatial audio in virtual reality: A systematic review. In *Proceedings of the 25th Symposium on Virtual and Augmented Reality*, pages 264–268, 2023. 1
- [9] Dima Damen, Hazel Doughty, Giovanni Maria Farinella, Sanja Fidler, Antonino Furnari, Evangelos Kazakos, Davide Moltisanti, Jonathan Munro, Toby Perrett, Will Price, and Michael Wray. The epic-kitchens dataset: Collection, challenges and baselines. *IEEE Transactions on Pattern Analysis and Machine Intelligence (TPAMI)*, 43(11):4125–4141, 2021. 1
- [10] Google DeepMind. Veo. 2024. 1, 2
- [11] Hao-Wen Dong, Xiaoyu Liu, Jordi Pons, Gautam Bhattacharya, Santiago Pascual, Joan Serrà, Taylor Berg-Kirkpatrick, and Julian McAuley. Clipsonic: Text-to-audio synthesis with unlabeled videos and pretrained language-vision models. In *2023 IEEE Workshop on Applications of Signal Processing to Audio and Acoustics (WASPAA)*, pages 1–5. IEEE, 2023. 1
- [12] Alexandre Défossez, Jade Copet, Gabriel Synnaeve, and Yossi Adi. High fidelity neural audio compression. *arXiv preprint arXiv:2210.13438*, 2022. 15
- [13] Patrick Esser, Robin Rombach, and Bjorn Ommer. Taming transformers for high-resolution image synthesis. In *Proceedings of the IEEE/CVF conference on computer vision and pattern recognition*, pages 12873–12883, 2021. 4
- [14] Leonardo A Fanzeres and Climent Nadeu. Sound-to-imagination: An exploratory study on unsupervised crossmodal translation using diverse audiovisual data. *arXiv preprint arXiv:2106.01266*, 2021. 1
- [15] Songwei Ge, Taesung Park, Jun-Yan Zhu, and Jia-Bin Huang. Expressive text-to-image generation with rich text. In *Proceedings of the IEEE/CVF International Conference on Computer Vision*, pages 7545–7556, 2023. 2
- [16] Jort F Gemmeke, Daniel PW Ellis, Dylan Freedman, Aren Jansen, Wade Lawrence, R Channing Moore, Manoj Plakal, and Marvin Ritter. Audio set: An ontology and human-labeled dataset for audio events. In *2017 IEEE international conference on acoustics, speech and signal processing (ICASSP)*, pages 776–780. IEEE, 2017. 2
- [17] Kristen Grauman, Andrew Westbury, Eugene Byrne, Zachary Chavis, Antonino Furnari, Rohit Girdhar, Jackson Hamburger, Hao Jiang, Miao Liu, Xingyu Liu, Miguel Martin, Tushar Nagarajan, Ilija Radosavovic, Santhosh Kumar Ramakrishnan, Fiona Ryan, Jayant Sharma, Michael Wray, Mengmeng Xu, Eric Zhongcong Xu, Chen Zhao, Siddhant Bansal, Dhruv Batra, Vincent Cartillier, Sean Crane, Tien Do, Morrie Doulaty, Akshay Erapalli, Christoph Feichtenhofer, Adriano Fragomeni, Qichen Fu, Abraham Gebrelesiasie, Cristina González, James Hillis, Xuhua Huang, Yifei Huang, Wenqi Jia, Weslie Khoo, Jáchym Kolář, Satwik Kottur, Anurag Kumar, Federico Landini, Chao Li, Yanghao Li, Zhenqiang Li, Karttikeya Mangalam,

- Raghava Modhugu, Jonathan Munro, Tullie Murrell, Takumi Nishiyasu, Will Price, Paola Ruiz, Merey Ramazanov, Leda Sari, Kiran Somasundaram, Audrey Southerland, Yusuke Sugano, Ruijie Tao, Minh Vo, Yuchen Wang, Xindi Wu, Takuma Yagi, Ziwei Zhao, Yunyi Zhu, Pablo Arbeláez, David Crandall, Dima Damen, Giovanni Maria Farinella, Christian Fuegen, Bernard Ghanem, Vamsi Krishna Ithapu, C. V. Jawahar, Hanbyul Joo, Kris Kitani, Haizhou Li, Richard Newcombe, Aude Oliva, Hyun Soo Park, James M. Rehg, Yoichi Sato, Jianbo Shi, Mike Zheng Shou, Antonio Torralba, Lorenzo Torresani, Mingfei Yan, and Jitendra Malik. Ego4d: Around the world in 3,000 hours of egocentric video. In *Proceedings of the IEEE/CVF Conference on Computer Vision and Pattern Recognition (CVPR)*, pages 18995–19012, 2022. [1](#), [2](#), [3](#), [6](#), [8](#), [14](#)
- [18] Agrim Gupta, Lijun Yu, Kihyuk Sohn, Xiuye Gu, Meera Hahn, Li Fei-Fei, Irfan Essa, Lu Jiang, and José Lezama. Photorealistic video generation with diffusion models. *arXiv preprint arXiv:2312.06662*, 2023. [1](#)
- [19] Wangli Hao, Zhaoxiang Zhang, and He Guan. Cmcgan: A uniform framework for cross-modal visual-audio mutual generation. In *Proceedings of the AAAI conference on artificial intelligence*, 2018. [1](#), [3](#)
- [20] Jonathan Ho, Ajay Jain, and Pieter Abbeel. Denoising diffusion probabilistic models. *Advances in neural information processing systems*, 33:6840–6851, 2020. [1](#), [2](#), [6](#), [15](#)
- [21] Joanna Hong, Minsu Kim, and Yong Man Ro. Visagesyntalk: Unseen speaker video-to-speech synthesis via speech-visage feature selection. In *European Conference on Computer Vision*, pages 452–468. Springer, 2022. [1](#)
- [22] Rongjie Huang, Jiawei Huang, Dongchao Yang, Yi Ren, Luping Liu, Mingze Li, Zhenhui Ye, Jinglin Liu, Xiang Yin, and Zhou Zhao. Make-an-audio: Text-to-audio generation with prompt-enhanced diffusion models. In *International Conference on Machine Learning*, pages 13916–13932. PMLR, 2023. [1](#), [2](#), [3](#), [6](#), [16](#)
- [23] Vladimir Iashin and Esa Rahtu. Taming visually guided sound generation. *arXiv preprint arXiv:2110.08791*, 2021. [1](#), [3](#)
- [24] Felix Kreuk, Gabriel Synnaeve, Adam Polyak, Uriel Singer, Alexandre Défossez, Jade Copet, Devi Parikh, Yaniv Taigman, and Yossi Adi. Audiogen: Textually guided audio generation. *arXiv preprint arXiv:2209.15352*, 2022. [2](#), [3](#)
- [25] Seung Hyun Lee, Wonseok Roh, Wonmin Byeon, Sang Ho Yoon, Chanyoung Kim, Jinkyu Kim, and Sangpil Kim. Sound-guided semantic image manipulation. In *Proceedings of the IEEE/CVF conference on computer vision and pattern recognition*, pages 3377–3386, 2022. [1](#)
- [26] Tingle Li, Yichen Liu, Andrew Owens, and Hang Zhao. Learning visual styles from audio-visual associations. In *European Conference on Computer Vision*, pages 235–252. Springer, 2022. [1](#)
- [27] Yuheng Li, Haotian Liu, Qingyang Wu, Fangzhou Mu, Jianwei Yang, Jianfeng Gao, Chunyuan Li, and Yong Jae Lee. Gligen: Open-set grounded text-to-image generation. In *Proceedings of the IEEE/CVF Conference on Computer Vision and Pattern Recognition*, pages 22511–22521, 2023. [2](#)
- [28] Kevin Qinghong Lin, Jinpeng Wang, Mattia Soldan, Michael Wray, Rui Yan, Eric Z Xu, Difei Gao, Rong-Cheng Tu, Wenzhe Zhao, Weijie Kong, et al. Egocentric video-language pretraining. *Advances in Neural Information Processing Systems*, 35:7575–7586, 2022. [1](#)
- [29] Yixin Liu, Kai Zhang, Yuan Li, Zhiling Yan, Chu-jie Gao, Ruoxi Chen, Zhengqing Yuan, Yue Huang, Hanchi Sun, Jianfeng Gao, et al. Sora: A review on background, technology, limitations, and opportunities of large vision models. *arXiv preprint arXiv:2402.17177*, 2024. [1](#), [2](#)
- [30] Simian Luo, Chuanhao Yan, Chenxu Hu, and Hang Zhao. Diff-foley: Synchronized video-to-audio synthesis with latent diffusion models. *Advances in Neural Information Processing Systems*, 36, 2024. [1](#), [2](#), [3](#), [6](#), [8](#), [15](#), [16](#)
- [31] Sagnik Majumder, Ziad Al-Halah, and Kristen Grauman. Learning spatial features from audio-visual correspondence in egocentric videos. *CVPR*, 2024. [1](#), [3](#)
- [32] Xiaqing Pan, Nicholas Charron, Yongqian Yang, Scott Peters, Thomas Whelan, Chen Kong, Omkar Parkhi, Richard Newcombe, and Yuheng Carl Ren. Aria digital twin: A new benchmark dataset for egocentric 3d machine perception. In *Proceedings of the IEEE/CVF International Conference on Computer Vision*, pages 20133–20143, 2023. [1](#)
- [33] Nathanaël Perraudin, Peter Balazs, and Peter L Søndergaard. A fast griffin-lim algorithm. In *2013 IEEE workshop on applications of signal processing to audio and acoustics*, pages 1–4. IEEE, 2013. [1](#), [3](#), [6](#), [14](#)

- [34] Nathanaël Perraudin, Peter Balazs, and Peter L Søndergaard. A fast griffin-lim algorithm. In *2013 IEEE workshop on applications of signal processing to audio and acoustics*, pages 1–4. IEEE, 2013. 6
- [35] Senthil Purushwalkam, Sebastia Vicenc Amengual Gari, Vamsi Krishna Ithapu, Carl Schissler, Philip Robinson, Abhinav Gupta, and Kristen Grauman. Audio-visual floorplan reconstruction. In *Proceedings of the IEEE/CVF International Conference on Computer Vision*, pages 1183–1192, 2021. 8, 15
- [36] Alec Radford, Jong Wook Kim, Chris Hallacy, Aditya Ramesh, Gabriel Goh, Sandhini Agarwal, Girish Sastry, Amanda Askell, Pamela Mishkin, Jack Clark, et al. Learning transferable visual models from natural language supervision. In *International conference on machine learning*, pages 8748–8763. PMLR, 2021. 3, 4
- [37] Aditya Ramesh, Mikhail Pavlov, Gabriel Goh, Scott Gray, Chelsea Voss, Alec Radford, Mark Chen, and Ilya Sutskever. Zero-shot text-to-image generation. In *International conference on machine learning*, pages 8821–8831. Pmlr, 2021. 2
- [38] Robin Rombach, Andreas Blattmann, Dominik Lorenz, Patrick Esser, and Björn Ommer. High-resolution image synthesis with latent diffusion models. In *Proceedings of the IEEE/CVF conference on computer vision and pattern recognition*, pages 10684–10695, 2022. 1, 2, 4, 16
- [39] Olaf Ronneberger, Philipp Fischer, and Thomas Brox. U-net: Convolutional networks for biomedical image segmentation. In *Medical image computing and computer-assisted intervention—MICCAI 2015: 18th international conference, Munich, Germany, October 5-9, 2015, proceedings, part III 18*, pages 234–241. Springer, 2015. 4
- [40] Flavio Schneider, Ojasv Kamal, Zhijing Jin, and Bernhard Schölkopf. Moûsai: Efficient text-to-music diffusion models. 2023. 2
- [41] Roy Sheffer and Yossi Adi. I hear your true colors: Image guided audio generation. In *ICASSP 2023-2023 IEEE International Conference on Acoustics, Speech and Signal Processing (ICASSP)*, pages 1–5. IEEE, 2023. 1, 2, 3, 6, 16
- [42] Uriel Singer, Adam Polyak, Thomas Hayes, Xi Yin, Jie An, Songyang Zhang, Qiyuan Hu, Harry Yang, Oron Ashual, Oran Gafni, et al. Make-a-video: Text-to-video generation without text-video data. *arXiv preprint arXiv:2209.14792*, 2022. 1, 2
- [43] Arjun Somayazulu, Sagnik Majumder, Changan Chen, and Kristen Grauman. Activerir: Active audio-visual exploration for acoustic environment modeling. *arXiv preprint arXiv:2404.16216*, 2024. 8, 15
- [44] Jiaming Song, Chenlin Meng, and Stefano Ermon. Denoising diffusion implicit models. *arXiv preprint arXiv:2010.02502*, 2020. 1, 2
- [45] Kun Su, Xiulong Liu, and Eli Shlizerman. Audeo: Audio generation for a silent performance video. *Advances in Neural Information Processing Systems*, 33: 3325–3337, 2020. 1, 3
- [46] Kun Su, Kaizhi Qian, Eli Shlizerman, Antonio Torralba, and Chuang Gan. Physics-driven diffusion models for impact sound synthesis from videos. In *Proceedings of the IEEE/CVF Conference on Computer Vision and Pattern Recognition*, pages 9749–9759, 2023. 1
- [47] Kim Sung-Bin, Arda Senocak, Hyunwoo Ha, Andrew Owens, and Tae-Hyun Oh. Sound to visual scene generation by audio-to-visual latent alignment. In *Proceedings of the IEEE/CVF Conference on Computer Vision and Pattern Recognition*, pages 6430–6440, 2023. 1
- [48] Arash Vahdat and Jan Kautz. Nvae: A deep hierarchical variational autoencoder. *Advances in neural information processing systems*, 33:19667–19679, 2020. 2
- [49] Shih-Lun Wu, Chris Donahue, Shinji Watanabe, and Nicholas J Bryan. Music controlnet: Multiple time-varying controls for music generation. *arXiv preprint arXiv:2311.07069*, 2023. 2, 13
- [50] Peng Xu, Xiatian Zhu, and David A Clifton. Multi-modal learning with transformers: A survey. *IEEE Transactions on Pattern Analysis and Machine Intelligence*, 2023. 1
- [51] Zeyue Xue, Guanglu Song, Qiushan Guo, Boxiao Liu, Zhuofan Zong, Yu Liu, and Ping Luo. Raphael: Text-to-image generation via large mixture of diffusion paths. *Advances in Neural Information Processing Systems*, 36, 2024. 2
- [52] Zhengyuan Yang, Jianfeng Wang, Zhe Gan, Linjie Li, Kevin Lin, Chenfei Wu, Nan Duan, Zicheng Liu, Ce Liu, Michael Zeng, et al. Reco: Region-controlled text-to-image generation. In *Proceedings of the IEEE/CVF Conference on Computer Vision and Pattern Recognition*, pages 14246–14255, 2023. 2
- [53] Lvmin Zhang, Anyi Rao, and Maneesh Agrawala. Adding conditional control to text-to-image diffusion models. In *Proceedings of the IEEE/CVF International*

Conference on Computer Vision, pages 3836–3847, 2023. [1](#), [5](#), [6](#), [13](#), [15](#)

- [54] Yongshuo Zong, Oisin Mac Aodha, and Timothy Hospedales. Self-supervised multimodal learning: A survey. *arXiv preprint arXiv:2304.01008*, 2023. [1](#)

EGOSONICS - SUPPLEMENTARY

A. EgoSonics

B. Synchronet

We propose *Synchronet*, a model to learn the correspondence between audio and video modalities by learning correlation between the input video embeddings and the audio frequencies for every time step t . ControlNet [53] is a current state-of-the-art neural network architecture that was introduced to enhance large pretrained text-to-image diffusion models with spatially localized, task specific image conditions providing pixel-level control. Over the time, ControlNet has been shown to work for a variety of controlled image generation tasks including but not limited to spatial conditions like *Canny edges*, *Hough lines*, *user scribbles*, *human key points*, *segmentation maps*, *shape normals*, *depths*, *cartoon line drawings*, etc. ControlNet basically works by processing these spatial conditioning and injecting additional control signals to the pretrained diffusion models. However, generating time-aware control signals to guide the output in temporally consistent manner has not been extensively studied using ControlNet. In fact, to the best of our knowledge, only Music ControlNet [49] uses it to generate partially-specified time-varying control signals. In this paper, we modified the ControlNet architecture to operate over given video embedding in both encoded feature space, and time space to generate control signals that can provide local pixel-level control to the Stable Diffusion’s UNet model to generate time-consistent audio spectrograms E_A . The generated spectrograms possess a strong correlation with the input video embedding and this results in highly synchronized audio of daily activity videos - where most previous methods fail due to design constraints.

We use *Synchronet* to provide control signals to Stable Diffusion (SD) 2.1. As a first step, we make a trainable copy of the entire UNet based encoder of SD along with the middle block and initialized them with the same pretrained weights of SD 2.1. The goal here is to use these trainable encoder to generate control signals that can be plugged into the pretrained SD’s UNet decoder blocks providing pixel-level control to output (see Fig. 6). The trainable copy is connected to the frozen SD through zero convolution layers to avoid any influence of noisy control signals during the start of the training.

Similar to ControlNet, the input conditioning image (E_V) of size 512×512 is converted to a feature space of size 64×64 , that matches the feature space of Stable Diffusion, through a pre-trained image encoder ϵ . We used the same convolution based image encoder as used in [53], and initialized it with the same weights. The image encoder is kept frozen throughout the training. The encoder ϵ extracts a feature space vector c_f from the input conditioning E_V .

As shown in Fig. 6, the noisy sample x is generated through forward diffusion process, where the input audio spectrogram of size 512×512 is encoded to a feature vector of size 64×64 through pre-trained VAE encoder. We used the same pretrained VAE encoder-decoder network as SD and initialized them with the same weights. Noise is added to the feature vector to get a noisy sample x for $T = 1000$ steps. Then the encoded video embedding $\epsilon(E_V)$ is added to the input noisy data sample x . $h = x + \epsilon(E_V)$. The added sum is further enriched by passing it through a self-attention block.

$$Self - Attn(Q_h, K_h, V_h) = Softmax\left(\frac{Q_h K_h^T}{\sqrt{d_K}}\right) V_h \quad (5)$$

$$h = h + Self - Attn(Q_h, K_h, V_h)$$

where, Q_h, K_h, V_h represents the Query, Key, and Value matrices derived from h . As we have seen in Table 3, only using this self attention block alone is sufficient to generate good quality audio spectrograms with an FID of 34.33. However, as the alignment score suggests, this alone is not sufficient to guide the diffusion model generate temporally consistent synchronized audio.

Thus, to inject the temporal consistency to the control signals of *Synchronet*, we also apply the cross-attention between the original video embedding E_V and h to guide the audio spectrogram generation directly with the time steps of E_V . This helps the model effectively learn the synchronization between the time domain and the rich feature space of Stable Diffusion, as we can see through a significant improvement in the alignment score. There are two options to apply cross-attention, either by using Query from E_V and Key and Value matrices from h , or vice-versa. In our case, we use the latter approach as follows:

$$Cross - Attn(Q_h, K_V, V_V) = Softmax\left(\frac{Q_h K_V^T}{\sqrt{d_K}}\right) V_V \quad (6)$$

$$h = h + Cross - Attn(Q_h, K_V, V_V)$$

where, Q_h, K_V, V_V represents the Query, Key, and Value matrices derived from h and E_V , respectively. After passing through a *linear layer*, a *zero convolution* layer is applied to get the control signal c^n .

The Stable Diffusion’s UNet architecture contains 12 encoder, 12 decoder and 1 middle blocks. Similar to [53], our trainable copy contains 12 encoder and 1 middle block consisting of several Vision Transformers (ViTs). Self-attention and cross-attention is applied in all the Spatial Transformers of encoder and middle blocks as described in algorithm 1.

These control signals are added to the 12 skip-connections and 1 middle block of the Stable Diffusion’s UNet decoder

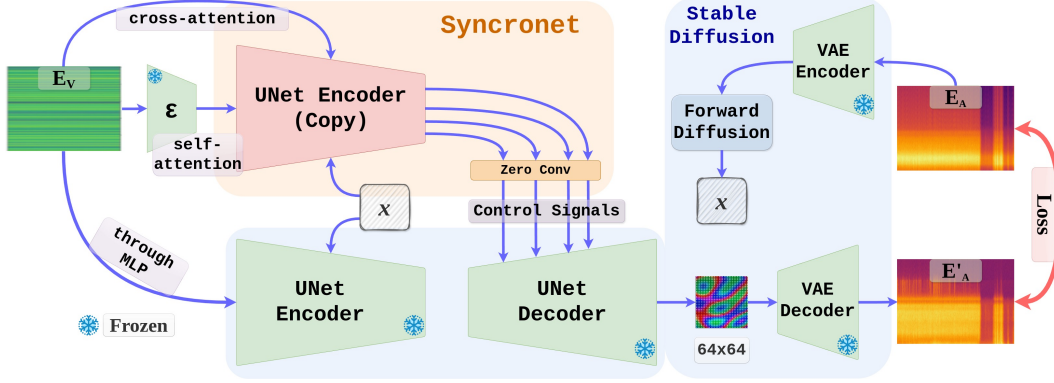


Figure 6. *Synchronet* training.

Algorithm 1 Generate Control Signals

Require: x : Input Noisy Sample
Require: EV : Video Embedding
Require: $timesteps$: Timestep tensor
Ensure: $control_signals$: List of control signals

- 1: $t_emb \leftarrow timestep_embedding(timesteps)$
- 2: $emb \leftarrow time_embed(t_emb)$
- 3: $context \leftarrow EV$
- 4: $guided_hint \leftarrow encoder(EV)$
- 5: $control_signals \leftarrow []$
- 6: $h \leftarrow x$
- 7: **for** $(module, zero_conv) \in (UNet.encoder_blocks, Synchronet.zero_convs)$ **do**
- 8: **if** $module == UNet.encoder_blocks.first_block$ **then**
- 9: $h \leftarrow module(h)$
- 10: $h \leftarrow h + guided_hint$
- 11: $guided_hint \leftarrow \text{None}$
- 12: **else**
- 13: **if** $module$ is `TimeStepBlock` **then**
- 14: $h \leftarrow module(h, emb)$
- 15: **else if** $module$ is `SpatialTransformer` **then**
- 16: {Apply self-attention and cross-attention}
- 17: $h \leftarrow module(h, context)$
- 18: **end if**
- 19: **end if**
- 20: Append $zero_conv(h, emb, context)$ to $control_signals$
- 21: **end for**
- 22: $h \leftarrow UNet.middle_block(h, emb, context)$
- 23: Append $zero_conv(UNet.middle_block_out(h, emb, context))$ to $control_signals$
- 24: **return** $control_signals$

block providing local pixel-level guidance at 64×64 , 32×32 , 16×16 , 8×8 resolutions.

C. Dataset and Training

Ego4D [17] is a large scale multimodal dataset consisting of around 3600 hours of daily activity videos. However, not every video in the dataset comes with corresponding audio, due to privacy concerns or technical limitations. Only half of the dataset has the corresponding audio. Now, when we look at the dataset, it contains a large amount of person-to-person conversations in shops, homes, outdoor scenes, etc., which doesn't serve any purpose in our use case. Thus, we only selected those videos that belongs to certain categories like *cooking*, *carpentry*, *laundry*, *cleaning*, *working*, *farmer*, *mechanic*, *yardwork*, *blacksmith*, etc. We believe, only such categories are useful in learning corresponding between audio and video for day-to-day activities. Even, in these videos, not every section of the video is important as there's a lot of redundancy in the data. To overcome this limitation, we calculate the Root Mean Square (RMS) value of a 10 second clip randomly picked from the dataset as follows:

$$S_{RMS} = \sqrt{\frac{1}{N} \sum_{i=1}^N x_i^2}$$

where, N is the total number of samples in audio waveform, and x is the value of each sample. After calculating the RMS value of each 10 second long audio sample, we compared it against a manually set threshold. If the sample's RMS value exceeded the threshold, we used it for training. This gave us a rich set of audio-video pair containing daily activities. We randomly picked a non-overlapping set of 150K such samples, which were used for training. Each 10 seconds long video is sampled at 30 frames per second and contains 300 frames in total. The corresponding audio is sampled at 22KHz, and converted to audio spectrogram using Short-Time Fourier Transform [33]. The audio spectrogram is resized to 512×512 from 430×1024 to make it compatible with Stable Diffusion's encoder-decoder network.

To get a more useful and compact video representation, we use video embedding as the representation of videos.

Video embedding is a feature rich image-like representation of the video where each video frame is represented as a vertical vector of shape 1×512 . 300 such vectors are placed one after the other in the same sequence as frame number to get the video embedding of shape 300×512 . Each video embedding is resized to 512×512 using bicubic interpolation to make sure it aligns with each time-step in the audio spectrogram.

Training of *Synchronet* has been done using the same loss functions as ControlNet [53]. We use DDIM [20] for faster and consistent sampling. Upto 1000 time steps were used in the forward process, and 20 during the denoising. Training was done using AdamW optimizer with a learning rate of $1e-4$.

E. Audio Super-Resolution

To upsample the generated audio spectrograms E_A from a resolution of 512×512 to 512×1024 , we trained a small 5 layer Convolutional Neural Network (CNN) with 16, 32, 64, 64, 32, 1 output filters. Each layer is followed by ReLU activation and Batch Normalization. Sigmoid is used as the final activation to keep the values in $[0, 1]$. The model was trained using pairs of original audio spectrograms of shape 512×1024 , and their down sampled version of shape 512×512 using Mean Square Error (MSE) loss. Adam optimizer was used for the optimization and a learning rate of 0.001 was used. The model was trained for 10 epochs with a dataset of 200K audio samples.

F. Video Summarization

Video Summarization is a long studied task which involves providing a short summary of a scene in a given video. It has been widely accepted that the audio contains rich information about the scenes and can even provide sufficient cues to reconstruct a scene geometry [35, 43]. We leverage this fact that audio provides additional cues about the scene through the easily identifiable sounds associated to improve the video summarization task. Our aim is to incorporate the audio generated from our method alongside the input video frames, and observe an improvement in the prediction accuracy of corresponding scene summary. We used a very simple setup to test this hypothesis as presented in Fig. 7. The input video frames are encoded to a rich feature space using the pretrained CLIP encoder. Initially, when the toggle switch is in "OFF" state, the Convolutional Neural Network (CNN) takes the video embedding E_V as the input, along with a zero vector as audio embedding e_A , and predicts the text embedding c'_t . The ground truth text embedding is estimated using the one sentence text summary after passing it through the CLIP text encoder. Ego4D dataset provides short narrations describing the activity of the scene. We used these narrations as the scene summary. The CNN

is trained using MSE loss and the parameters are optimized using Adam optimizer with a learning rate of $5e^{-3}$.

When the toggle switch is "ON", that is, when the zero vector e_A is replaced with the GT audio embedding, the CNN takes in this additional input and concatenates it with the video embedding vector through convolution. Similar as before, the model tried to predict the text embedding and the CNN is trained until convergence. We use a well known audio compression method EnCodec [12] to encode the audio waveform into a more rich neural codec representation.

Once the model is trained, we compared its performance on the test dataset using various methods. The results are presented in Table 2.

G. Video-to-Text Embedding MLP

We trained a small two layer MLP that takes a normalized video embedding E_V , and generates a vector of shape 512, which acts as a text embedding c_t to the stable diffusion model. The MLP was trained using 200K pair of video and text embedding using MSE loss and Adam optimizer.

H. Synchronization Metrics

An effective way of measuring the audio-video alignment is missing in the field of audio-visual learning. Thus, inspired by Diff-Foley [30], we introduced a Vision Transformer based metrics (Alignment Score) that can calculate the synchronization between audio and video. Unlike Diff-Foley, we used ViT-B32 as a feature extractor to get audio features from E_A , and video features from E_V , and then use 5 Linear layers, each followed by a ReLU activation. We use a pre-trained ViT-B32 trained on *IMAGENET1K_V1*. The linear layers were trained using MSE loss and Adam optimizer with a learning rate of 0.0001. Our training dataset consists of 200K samples, out of which 100K were labelled as 1 and the remaining 100K as 0. Audio samples belonging to the same video were all labeled as 1 and accounts for 50% of the training data. 25% data is the audio samples randomly assigned with any video other than the original video. These were labeled as 0. Remaining 25% samples came from randomly shifting the audio anywhere between 1–5 seconds from the true audio-video pair. These were also labeled as 0. Our classifier reached an accuracy of 97% on testing dataset comprising of 20% of the training data kept separately. If the trained model classifies an audio-video pair as anything close to 1, it means the two modalities are accurately aligned. *EgoSonics* scores an average accuracy of 92% on test dataset meaning that we significantly outperforms the existing methods in better synchronizing audio.

For calculating Alignment Score (AS) at 15 FPS, we replaced the alternate image embeddings E_V^i with their previous ones E_V^{i-1} , to ensure its consistent with the trained model. Similarly, we did for testing at 4 FPS.

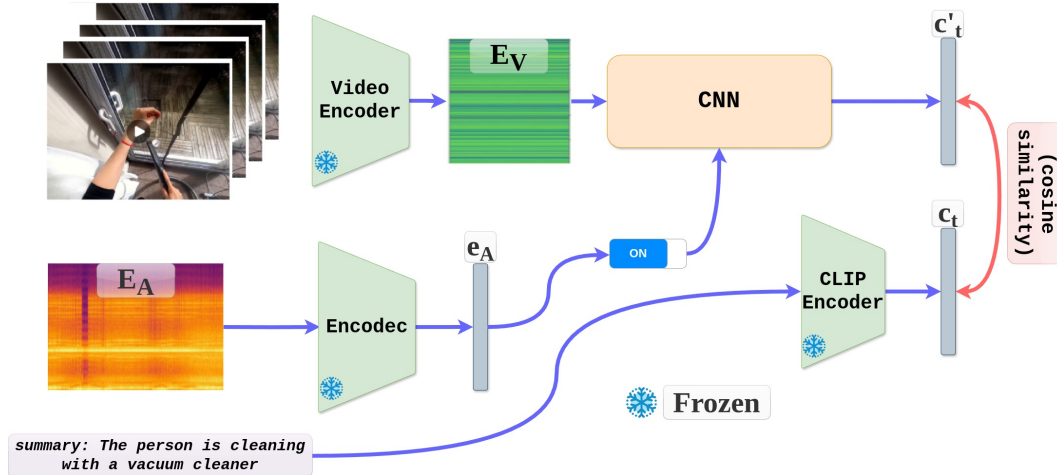


Figure 7. Video Summarization.

H. Comparison with Baselines.

We compared our model against 3 different baselines: Diff-Foley, Im2Wav, and Make-an-Audio [22, 30, 41]). Im2Wav samples the input audio at 16 KHz and generates an audio of length 5 seconds. Make-an-Audio also samples at 16 KHz, but generates an audio of length 9-10 seconds with the intermediate spectrogram representation of 80×624 . Diff-Foley also samples at 16 KHz to generate an audio of length 8 seconds via audio spectrogram of shape 256×128 . On the contrary, we samples the input audio waveform at a higher 22 KHz sampling rate and also generates longer audio samples of 10 seconds. Using Stable Diffusion [38] allowed us to generate high resolution spectrograms that can fit more frequency bins and longer temporal length. For calculating the metrics of baselines, we make sure to use the same length ground truth audio wave as they generate for a fair comparison. We fine-tuned the Im2Wav, Make-an-Audio, and Diff-Foley’s CAVP model for a few iterations on our dataset before testing.

I. More Results

Fig. 9 shows more results generated from our model. We have used a different color scheme for spectrograms for a different perspective.

J. Failure Cases, Limitations, and Ethical Considerations

We also analyzed the failure cases. Most of the failure cases can be classifier into two categories: temporal misalignment and context-level misalignment. The temporal misalignment refers to cases where the model is able to predict contextually meaning audio, however, it’s misaligned with the input video. Fig. 8(a) shows some of the misaligned

results. The main factor contribution to the misalignment is the lack of rich visual information is most cases. For example, in the first case, a carpenter is polishing a steel bar with a rotating brush and the sound is made when they both are in contact. However, from the video, it’s not very clear if the steel bar is actually in contact with the rotating brush or no.

The other type of failure happens when the model is not able to predict the contextually acceptable audio. This is mainly a reason of lack of data. For example, since there are a very few samples of musical instruments in the Ego4D dataset, our model doesn’t perform very well on such videos. The similar thing happens if the model encounters people interacting. We believe that such challenges can be solved by training our model on a large amount of dataset comprising millions of audio-video pairs.

EgoSonics, being a generative model capable of accurately predicting audio from muted video, should be restricted to applications in research, the development of interactive AR/VR technologies, and assistive technologies for individuals with impairments. It is imperative to enforce strict adherence to ethical guidelines to prevent the misuse of this model for unethical purposes.

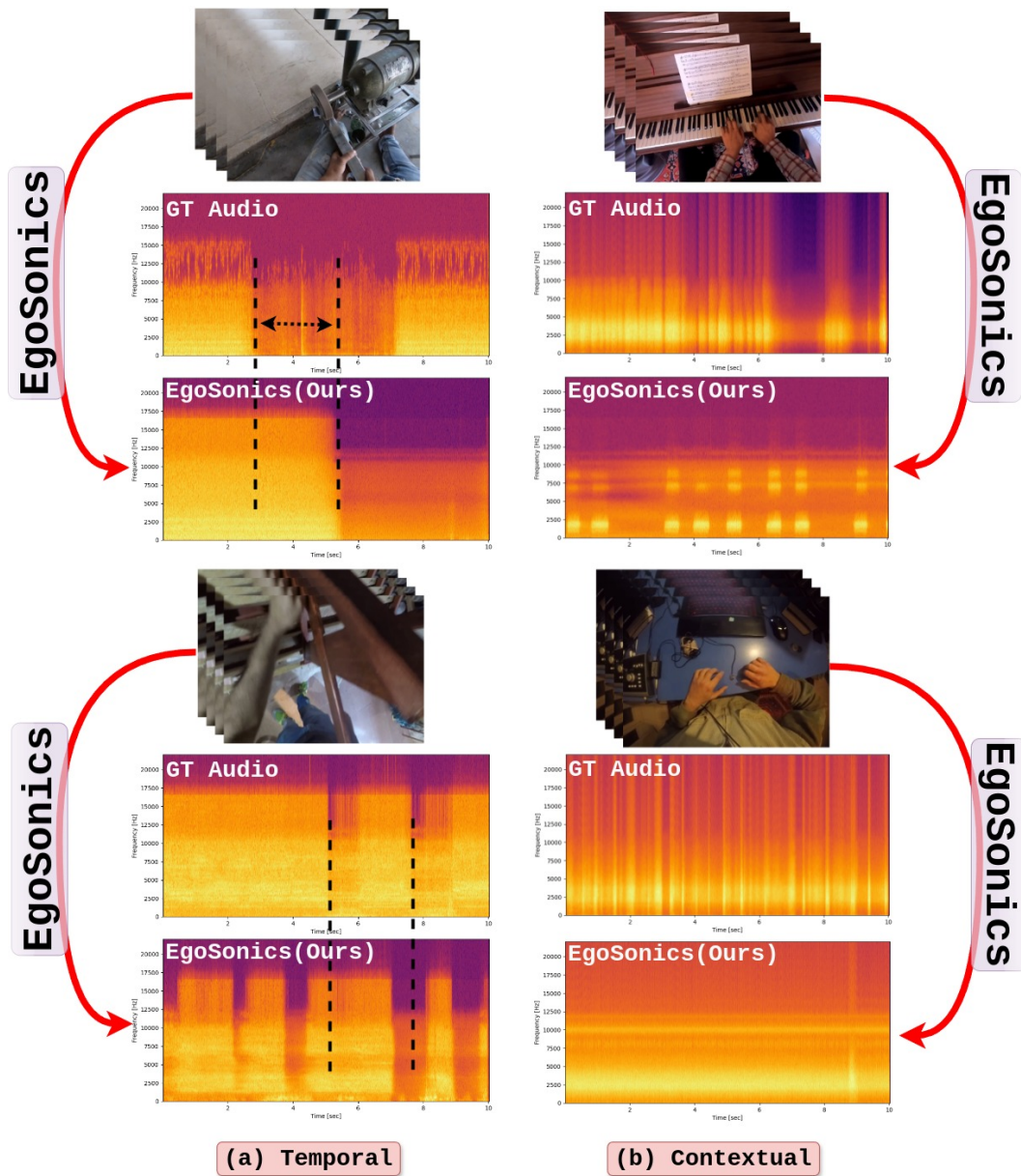


Figure 8. Failure Cases. There are two types of failure cases: (a) Temporal misalignment, (b) Contextual misalignment.

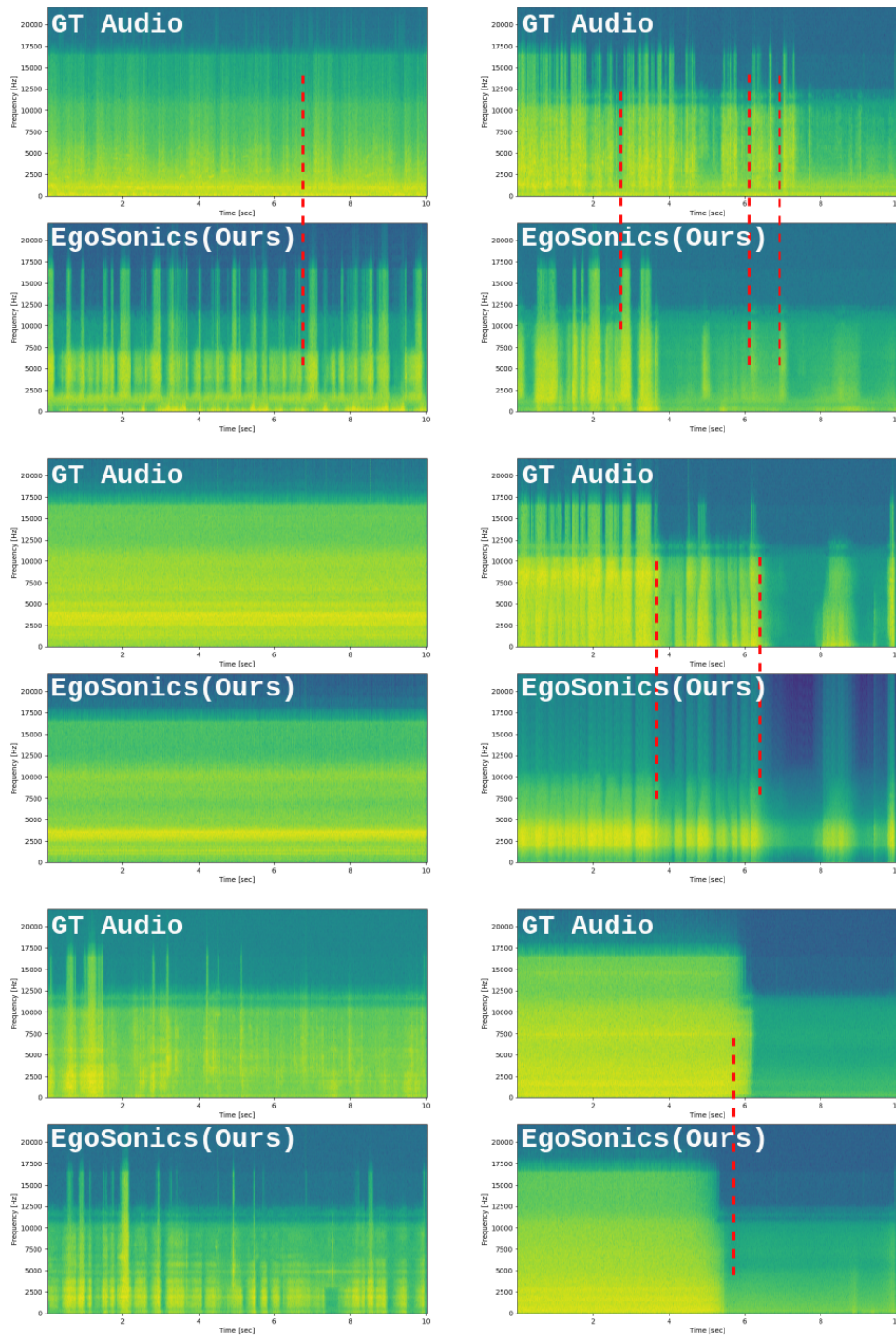


Figure 9. More Results (different color map).